Calculation of rotationally inelastic processes in electron collisions with CO_2 molecules

F. A. Gianturco[1] and T. Stoecklin[2]
[1]*Max-Planck-Institut für Strömungsforschung, Bunsenstraβe 6-10, 38173 Göttingen, Germany and Department of Chemistry, The University of Rome, Cittá Universitaria, 00185 Rome, Italy**
[2]*Laboratoire de Physico-chimie Theorique, 351 Cours de la Liberation, 35400, Talence, France*
(Received 16 September 1996)

The rotational excitation of the title linear polyatomic target, treated as a rigid rotor is computed using a fully *ab initio* interaction potential recently employed to obtain integral elastic cross sections [Gianturco and Stoecklin, J. Phys. B **29**, 3933 (1996)] and to unravel several resonances in the low-energy region. The present study looks at the rotationally inelastic processes which can occur in the energy range across the long-lived shape resonance at 3.9 eV and finds that the resonant process strongly enhances the overall efficiency of the rotational excitation by the electron projectile, as shown by the computed values of the average rotational energy transfers. Angular distributions are also evaluated at different collision energies and compared with earlier calculations. [S1050-2947(97)05602-3]

PACS number(s): 34.80.Gs

I. INTRODUCTION

In the analysis and interpretation of electron transport data from swarm experiments one needs to account for a broad variety of molecular excitations that can be induced by electron impact. In order to provide a realistic and global modeling of the experiments, in fact, one requires knowledge of the cross sections for some of these excitations so that the uncertainties which exist in the unfolding of other cross sections by transport analysis can be reduced [1,2]. The CO_2 molecule has been, and still is, one of the most popular systems for which the excitations of rotational and vibrational degrees of freedom play a very important role in the interpretation of electron transport phenomena [3]. The fact that its threshold for rotational excitation is quite low (typically of the order of less than 1 meV for small values of the final rotational quantum numbers) means also that considerable rotational excitation is possible even for fairly low impact energies of the electrons. Furthermore, the rotational excitation of this molecule is considered to be an important cooling mechanism in molecular gases and in the processes occurring in the planetary atmospheres [4,5]. We have recently carried out an extensive set of calculations for the elastic (rotationally summed) integral and differential cross sections over the low-energy scattering region and across the strong shape resonance of this system [6]. It therefore becomes of interest to further extend such a study, which turned out to provide a very good agreement between experimental and theoretical quantities, to the behavior of the rotationally inelastic processes, integral and differential cross sections, and to the evaluation of the overall efficiency of low-energy electrons in exciting rotational levels in the ground electronic state of the CO_2 target.

II. ROTATIONALLY INELASTIC SCATTERING

We briefly summarize our computational procedure and the calculations which we have carried out earlier on this system [6]. The actual details have been given before and therefore we will not repeat them here. The approach we used to solve the collision problem is as follows: The fixed-nuclei approximation (FNA) is made to treat the molecular degrees of freedom [7] and the target is taken to be a rigid rotor with the internuclear separation fixed at $R_{CO} = 2.1944 a_0$. Furthermore, only the ground electronic state is retained in the eigenfunction expansion of the target scattering wave function. The coupled scattering equations are formulated in a single-center expansion (SCE) body-fixed (BF) coordinate system [6], converted to integral equations [8], and solved by numerical quadrature. In all the calculations, as discussed earlier [6,9], care was taken in treating the partial-wave expansion of the scattering function and the expansion of the potential energy in Legendre polynomials in ways for which enough terms are included to ensure convergence to better than 5% in the resulting cross sections [6,9].

The electron-molecule interaction potential is given by the sum of three main contributions: the *ab initio* static term generated from the electronic density of the target wave function, the exchange interaction given by a separable expansion over an additional set of discrete functions [10], as described earlier by us [6], and the correlation polarization (V_{CP}) interaction, which describes the response of the target charge distribution to the impinging $(N+1)$st electron. In the short region this function is obtained from a density-functional (DF) modeling of the dynamic correlation [11,12] while the long-range part describes the polarization effects through the static dipole polarizabilities of the target molecule [13]. The resultant calculated elastic integral cross sections (rotationally summed) and the corresponding momentum-transfer integral cross sections turned out to be in quite good agreement with the measured results [6] and exhibited the correct trends with energy, including the unusually steep rise of it as the energy decreases below about 1.0 eV.

It therefore seemed reasonable to further employ the computed T-matrix elements obtained from the FNA treatment to

*Present address and address for correspondence.

generate the corresponding rotational cross sections, elastic and inelastic, integral and differential, over the same broad range of collision energies. From the theoretical standpoint, in fact, one can obtain such cross sections by employing the same FNA T-matrix elements and transforming them into a space-fixed (SF) laboratory reference frame via the appropriate unitary transformations [13,14], which, for Σ states of the target, are given by

$$T^J_{j\ell,j'\ell'}=(-)^{\ell+\ell'}\sum_m C(J,\ell,j;-m,m) \times C(J,\ell',j';-m,m)T^m_{\ell\ell'}, \quad (1)$$

where the C's are the usual Clebsch-Gordan coefficients. This result can be used to calculate state-to-state, rotationally inelastic cross sections from an initial state j to a final state j' [15]

$$\sigma(j\to j')=\frac{\pi}{k_j^2(2j+1)}\sum_J (2J+1)\sum_{\ell\ell'}|T^J_{j\ell,j'\ell'}|^2, \quad (2)$$

which has been averaged over initial m_j sublevels and summed over final $m_{j'}$ sublevels. From the FNA scheme we ignore the rotational level spacings an therefore one sets $k_j^2=k^2$ for all j. Here k^2 is the scattering energy in Rydberg. From the FNA T-matrix elements one therefore obtains the final formula of the state-to-state partial integral cross sections

$$\sigma(j\to j')=\frac{\pi}{k^2(2j+1)}\sum_J (2J+1)\sum_{\ell\ell'}\sum_{m,m'} \times C(J,\ell,j;-m,m)C(J,\ell',j';-m,m) \times C(J,\ell,j;-m',m')C(J,\ell',j';-m',m') \times\{T^{(R)m}_{\ell\ell'}T^{(R)m'}_{\ell\ell'}+T^{(I)m}_{\ell\ell'}T^{(I)m'}_{\ell\ell'}\}, \quad (3)$$

where the $T^{(R)}$ and $T^{(I)}$ are the real and imaginary parts of the FNA, body-frame (BF) T-matrix elements $T^m_{\ell\ell'}$ of Eq. (1). Due to the unitary nature of the transformation (1), the total integrated cross section is invariant under this transformation of the T operator and therefore we can also write

$$\sigma_{\rm tot}=\frac{\pi}{k^2}\sum_{\ell\ell'}\sum_m |T^m_{\ell\ell'}|^2=\sum_{j'}\sigma(j\to j'), \quad (4)$$

which is independent of j. The last two equations are the usual application of the adiabatic-nuclei-rotational (ANR) approximation, whereby the rotationally inelastic processes are obtained by an adiabatic transformation [14] of the fixed-nuclei matrix elements after the dynamics has been already completed without any explicit inclusion of nuclear rotational coupling with the impinging electron [16] during the scattering process. Such an approximation can be considered valid for e^--CO_2 scattering collisions in the energy range under consideration (from 0.5 up to 30 eV), since the spacing of adjacent low-lying rotational levels in the ground vibronic state of CO_2 is of the order of 0.1 meV. On the other hand, it may not be quantitatively correct close to the energy position of the shape resonance [6].

It is also interesting to note that the corresponding inelastic, state-to-state differential cross sections can be written in a similar way as

$$\frac{d\sigma}{d\Omega}(j\to j')=\frac{1}{4k^2(2j+1)}\sum_L A_L^{j,j'}(E)P_L(\cos\theta), \quad (5)$$

where θ is now the SF scattering angle and the A_L coefficients are given, at each scattering energy E, by a well-known set of formulas already discussed several times in the literature for linear molecules [15,17,18]. They will not be repeated here, where it suffices to say that the A_L's are a direct function of the $T^m_{\ell\ell'}$, of Eq. (1), transformed into the SF frame by that equation and by the use of the ANR approximation [14] already employed to compute the T-matrix elements.

Similar types of calculations were carried out long ago by Morrison and Lane [19] using an entirely empirical treatment of both exchange and polarization forces. The same system was also discussed by Truhlar and co-workers [20,21] from the point of view of rotationally inelastic collisions by using a model effective-potential approach. Only one energy value (20 eV) was examined in their first work, while further calculations with the same method were later carried out at 10 eV [21]. In the last two references the calculations were performed in the SF frame of reference by rotational close-coupling expansions and angular distributions were also presented for some of the rotational excitation processes from the lowest-j level as the initial molecular level.

The results from the present calculations and a comparison with the previous theoretical applications will be discussed and analyzed in the following section.

III. COMPUTATIONAL RESULTS

A. Partial integral cross sections

As mentioned in the previous discussion, the evaluation of the ANR inelastic cross sections (even across the resonance region for the title molecule) is likely to be a reasonable approach for the CO_2 target given the smallness of the rotational spacings between the lower j' excited states. Furthermore, the rotational excitation of nonpolar targets at low collision energies is expected to be smaller than the corresponding elastic cross section $\sigma(j\to j)$ [22]. The results of Fig. 1, however, reveal a different behavior for the present system. We show there the partial integral cross sections, $\sigma(j\to j')$, starting from the $j=0$ level and in the energy range between 2.0 and 10.0 eV. One clearly sees there the following features.

(1) In the energy range between 2.0 and nearly 4.0 eV the $(0\to 2)$ inelastic cross section is nearly one order of magnitude larger than the elastic one and remains the strongest process at the resonance energy: only from about 4.5 eV the elastic process takes over, while the $\Delta j=2$ excitation still remains the largest excitation process.

(2) The resonance region corresponds to a very marked increase of all inelastic processes and confirms the strong

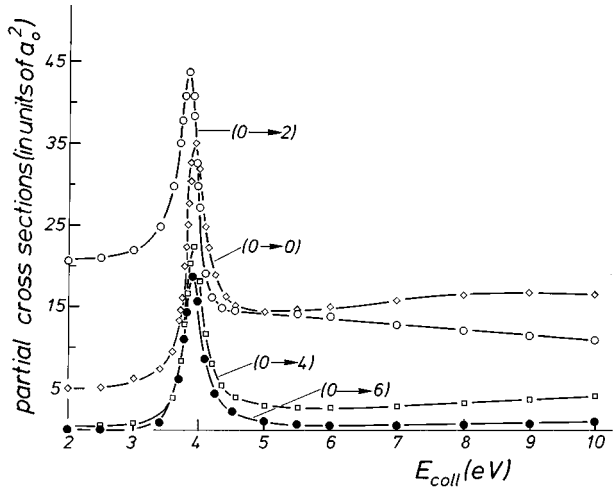

FIG. 1. Computed partial integral cross sections (a_0^2), as a function of collision energy, for rotational state-to-state processes ($j \rightarrow j'$). Open diamonds: (0→0); open circles: (0→2); open squares: (0→4); filled circles: (0→6).

partial-wave mixing in the interaction which causes the enhancement of the energy transfer mechanism during the collisional event.

That this partial ''inversion'' effect pertains to the (0→2) inelastic processes could be seen by the behavior of the elastic and inelastic cross sections which originate from the $j=2$ and $j=4$ levels and which are shown in Fig. 2. One sees there, in fact, that both elastic processes from these levels (upper and lower curves in the figure) are indeed dominating the scattering and yield the largest cross sections over the whole range of collision energies. Furthermore, the $\Delta j=2$ inelastic transitions are once more the ones with the largest cross sections, although markedly smaller than the elastic contributions. This result is in accord with what was found by the earlier model calculations [19], where the size of the cross sections was also obtained in close agreement with the present calculations. Since the resonance region is dominated by the Π_u symmetry [6,19] for which the contributing partial waves are $\ell=1$, 2, and 3 with a prevalence of d-wave effects, then the direct coupling (by the quadrupole term of the interaction) between the $j=0$ and $j'=2$ levels involved in that transition becomes particularly strong and effective in the low-energy region discussed here.

This also explains why the corresponding $\Delta j=2$ excitations are again the dominant inelastic processes even when the initial level is changed to $j=2$ or to 4, as seen in Fig. 2. This specific effect is also to be related to the dominant long-range interaction included in the present work, i.e., to the dipole static polarizability of CO_2 for the $\ell=2$ nonspherical component [23]. In such a case, in fact, the long-range interaction extends to the long-range region the same direct coupling induced by the resonance d wave in the short-range region and therefore reinforces the fact that the $\Delta j=2$ process is here the largest rotational excitation process [19]. When we consider the inelastic cross sections at 10 eV of collision energy, we find the $\sigma(0\rightarrow2)$ cross section to be about $13.0a_0^2$, i.e., fairly close to the earlier calculations [19] which gave $8.6a_0^2$ but markedly smaller than the value from Truhlar and co-workers [21] of $25.3a_0^2$. This relative difference is also present with the $\sigma(0\rightarrow4)$ inelastic cross section at the same energy, where we find a value of $5.0a_0^2$. The value of Morrison and Lane [19] is $3.7a_0^2$ while Truhlar and collaborators [21] find $11.1a_0^2$. Since we do not expect the ANR to be incorrect at such a high collision energy, the differences in the modeling of the interaction forces must be mainly responsible for such oscillations in the values of the computed inelastic cross sections. It is interesting to note that the earlier comparisons [21] with rotationally summed experiments suggested that the (0→2) inelastic process should have a cross section between $9.0a_0^2$ and $25.0a_0^2$, in agreement with our current estimate of $13a_0^2$. The same considerations also apply to the $\sigma(0\rightarrow4)$ inelastic process and find our present results in closer accord with experimental estimates [21].

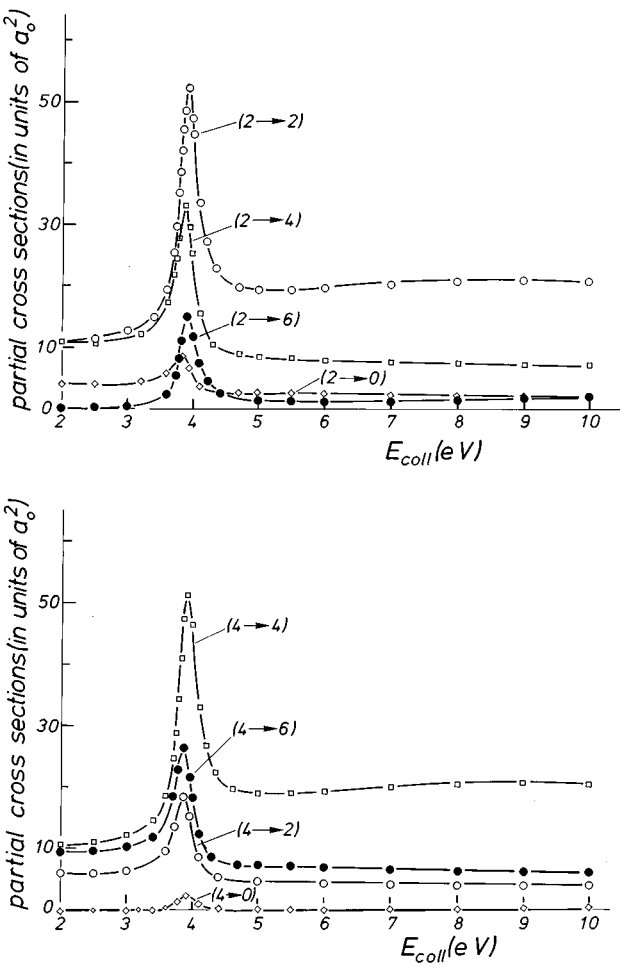

FIG. 2. Same as in Fig. 1 but for different initial rotational states of CO_2. Upper part: transitions from the $j=2$ level. Lower part: transitions from the $j=4$ level.

B. State-to-state inelasticity

When considering the general interest which exists in the cooling rates of CO_2 levels and their importance to estimate electron energy distribution functions for the title system one must also keep in mind that, as the gas temperature increases, the corresponding peak in the Maxwell-Boltzmann distribution function obviously moves to higher values of j. For instance, it is interesting to note that in CO_2 at $T=100$,

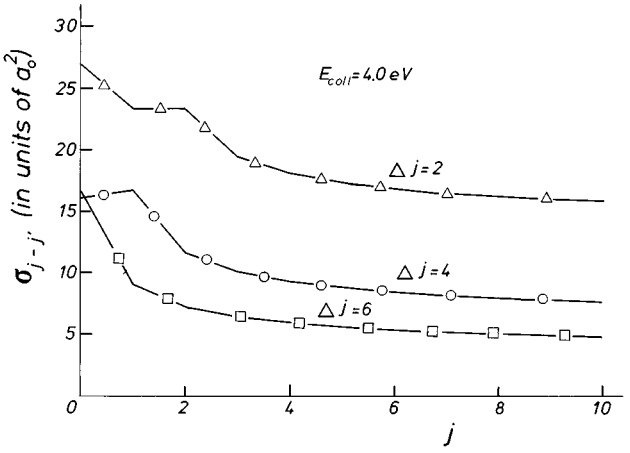

FIG. 3. Partial integral inelastic cross sections, at 4.0 eV of collision energy, as a function of the initial level j and for different transitions: $\Delta j=2$ (open triangles), $\Delta j=4$(open circles) and $\Delta j=6$ (open squares).

300, and 500 K the peaks move from $j=8$ to $j=16$ and 20, respectively. It therefore becomes important to evaluate the corresponding inelastic processes over a rather broad range of initial j values for the various excitation functions.

The present calculated values for initial j from 0 to 10 are shown, at the energy of the resonance discussed before, in Fig. 3. One clearly sees the following behavior.

(1) The $\Delta j=2$ excitation process is, at resonance, by far the largest excitation process.

(2) From the initial $j=4$ and higher the excitation is fairly independent of j, as expected from the ANR formulation, while small differences appear for $j=0$ and 2.

(3) The excitation processes with $\Delta j=4$ and 6 are also showing the same dependence on j and turn out to be close to each other in magnitude.

It is therefore useful to further analyze the excitation efficiency by looking at the same set of inelastic cross sections at different collision energies. As an example of this analysis, their behavior at E values right below and just above the resonance position is reported in Fig. 4. One sees that the excitation cross sections below the resonance position are a factor 2 smaller than those at the resonance for the $\Delta j=2$ processes, and have essentially vanished for excitations with larger $\Delta j=2$ values. This behavior is still more marked when one looks at the cross sections at the collision energy of 5.0 eV (lower part of Fig. 4). The excitation processes with $\Delta j=2$ have become even smaller: their average value in the nearly j-independent energy region above 4 eV is around $8a_0^2$ while it was more than $20.0a_0^2$ at the resonance energy (see Fig. 3). The main physical reason here seems to be the marked reduction of the $\ell=2$ contribution from that of the resonant cross sections as one moves away from the energy region of the Π_u resonance. We see, in fact, that the calculations at higher collision energies (shown in Fig. 5 for 10.0 and 20.0 eV) are essentially producing very similar inelastic cross sections to those obtained at 5.0 eV: the average value for the $\Delta j=2$ cross sections remains around $8.0a_0^2$ while that for the $\Delta j=4$ and 6 excitations increases to slightly larger values, although remaining always much smaller than the former excitations. The nearly constant nature of the results at large j values reflects the fact that, using the AN approximation, the ratio of the statistical weights of the initial and final state approach unity as $j\to\infty$.

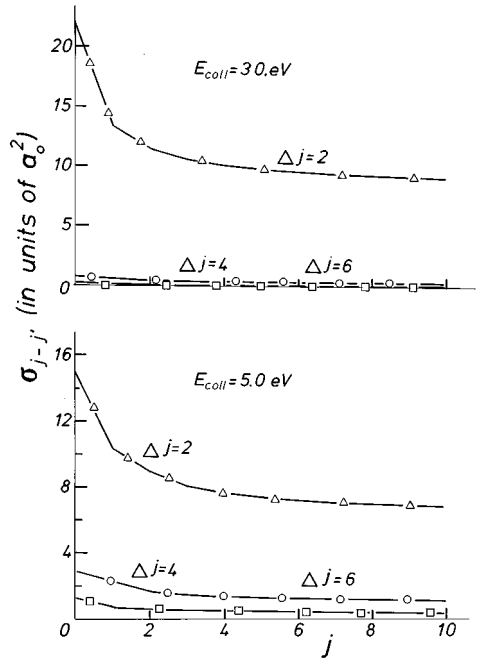

FIG. 4. Same as in Fig. 3 but for different values of collision energy. Top: for $E_{\rm coll}=3.0$ eV. Bottom: for $E_{\rm coll}=5.0$ eV. The meaning of all symbols is the same as in Fig. 3.

In conclusion, we can say that the present calculations show a marked increase of rotational efficiency at the resonance region, where the electron interacts with the target for a longer time, and that the direct dynamical coupling by d

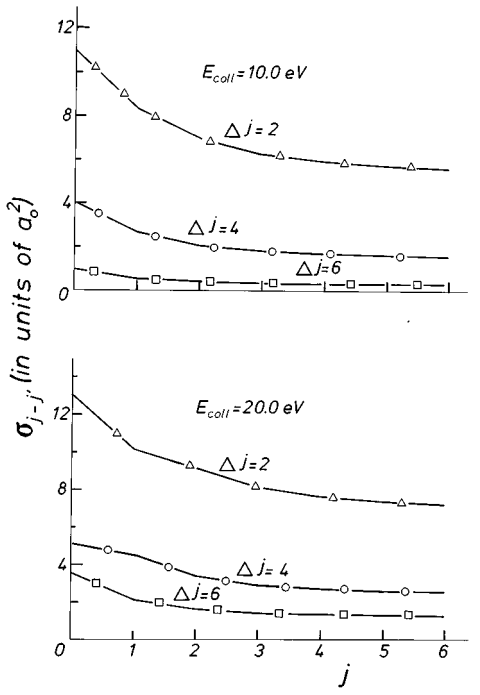

FIG. 5. Same as in Figs. 3 and 4 but for two more values of collision energy. Upper part: $E_{\rm coll}=10.0$ eV. Lower Part: $E_{\rm coll}=20.0$ eV.

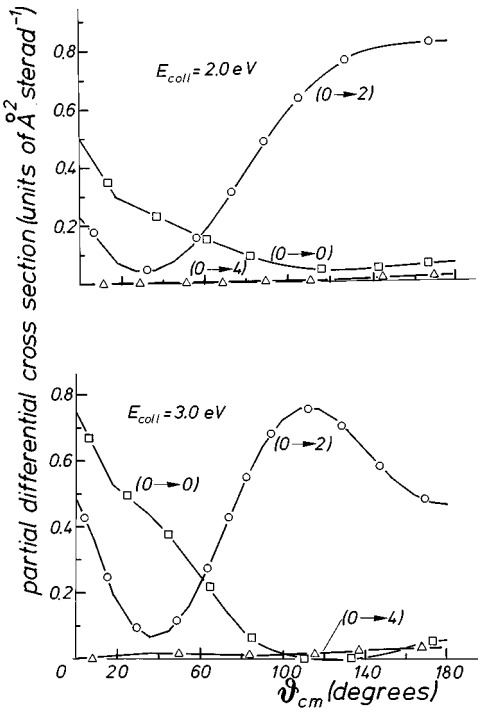

FIG. 6. Computed partial differential cross sections at different collision energies and for different transitions. Upper part: for $E_{\rm coll}=2.0$ eV. Lower part: $E_{\rm coll}=3.0$ eV. Open circles: (0→2) excitations; open squares: (0→0); open triangles: (0→4) transitions.

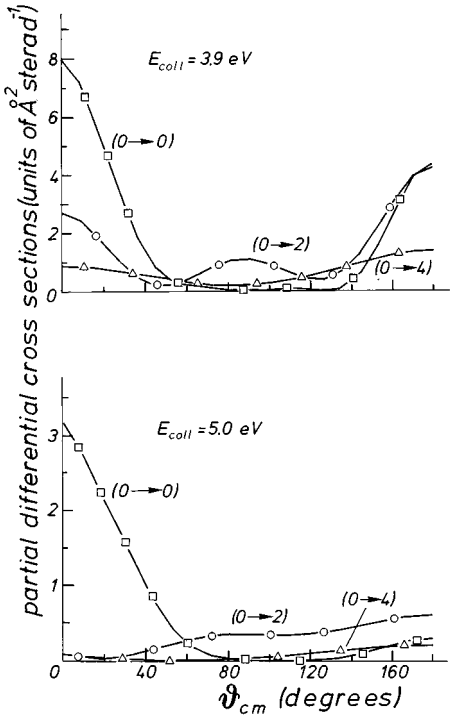

FIG. 7. Same as in Fig. 6 but for different collision energies. Upper part: 3.9 eV. Lower part: 5.0 eV.

waves for the $\Delta j=2$ transitions is also strongly enhanced in the resonance region.

These results are in accord with the earlier model calculations [19] where the inelastic cross sections showed a minor increase with increasing collision energy and where the average values were rather close to the present ones. On the other hand, the later model calculations [20] at 20 eV yield cross sections much larger than the present ones, in spite of our more accurate computational model. Their $\sigma(0\rightarrow2)$ cross section is shown to be $15.52a_0^2$ while ours is about $8.0a_0^2$. Likewise, their $\sigma(0\rightarrow4)$ and $\sigma(0\rightarrow6)$ cross sections are $8.34a_0^2$ and $8.46a_0^2$ at 20 eV, while our present calculations yield $3.5a_0^2$ and $2.7a_0^2$, respectively. It therefore appears that the interaction modeling of that work, or their convergence checks on the calculations, are inadequate to realistically describe rotational excitations in the present system.

C. Partial differential cross sections

The evaluation of angular distributions after inelastic collisions is also a very useful indicator of the forces at play and of the role played by the different coupling potential components during the dynamics. The only examples of computed rotationally inelastic cross sections are given at 10 eV [21] and at 20 eV [20], while we are not aware of any other calculation at lower collision energies, especially around the resonance region. We therefore decided to carry out such a set of calculations by starting with the collision energy below the resonance position.

Figure [6] reports the calculated quantities from Eq. (5), where the sum was carried out up to $L=38$ in the generation of the A_L coefficients. The results in the top part of the figure refer to 2.0 eV of collision energy, while those in the lower part correspond to differential cross sections (DCS) at a collision energy of 3.0 eV. As seen already when discussing partial, state-to-state integral cross sections, we detect a dominance of the (0→2) inelastic cross sections even over the elastic (0→0) process. As a result of it, the inelastic process makes the backward scattering dominate the summed DCS since the (0→0) process is mostly in the forward direction as expected for elastic scattering events. On the other hand, as we move near to the resonance region (Fig. 7) we see that the resonant excitation for $\Delta j=2$ clearly shows an $\ell=2$ angular distribution with symmetric intensity around 90°, as has been observed before for resonant angular scattering [24]. This feature rapidly disappears, however, as one moves to higher collision energies and the inelastic cross sections become smaller than the elastic ones. The latter process, therefore, dominates the scattering and the forward direction is the one contributing the most to the rotationally summed quantities. The $\Delta j=4$ processes appear to be rather small at both collision energies and also show little dependence on the scattering angle.

This general behavior is seen even more clearly as one moves to larger collision energies, away from the resonance feature: computed results at 10 and 20 eV are shown in Fig. 8 for the state-to-state DCS of the present system. Their behavior is rather constant with energy, in the sense that the elastic process is still the dominant one at both energies and that the forward scattering remains a constant feature of the rotationally summed cross sections. This result is in general accord with the earlier calculations [20,21] since they also showed that the elastic (0→0) DCS was mostly forward scattering. The specific features of the present, inelastic DCS are, however, rather different from theirs: our inelastic processes,

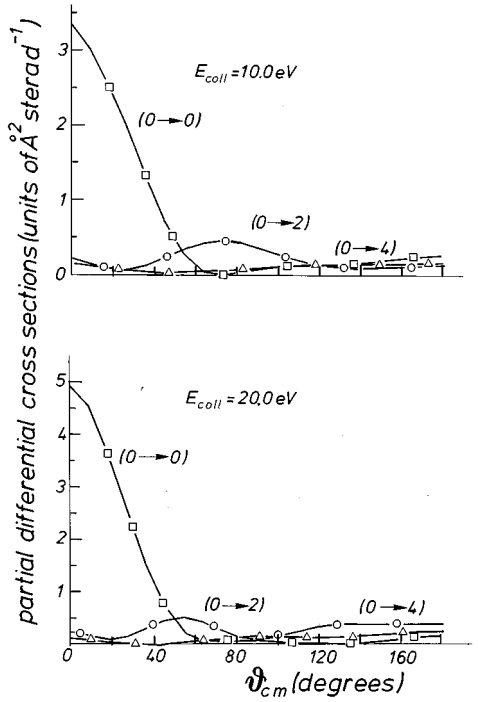

FIG. 8. Same as in Figs. 6 and 7 but for two further values of collision energies. Upper part: $E_{\rm coll}=10.0$ eV. Lower part: $E_{\rm coll}=20.0$ eV. The meaning of all symbols is the same as in the other two figures.

in fact, are much less oscillatory with angle and are larger than the earlier model results [20,21] in the region away from the forward scattering area. Here again we expect that the rather crude model employed by those calculations is not sufficient to realistically describe the short-range interaction in this polyatomic target.

D. Energy transfer efficiency

Because of the general interest in the present CO_2 molecule for cooling processes in the interstellar medium, it becomes useful to define a possible measure of its efficiency to be ''heated'' by collisions with electrons over a fairly broad range of scattering energies. Thus, we have computed, from the previous inelastic DCS, the following average energy transfer given at each fixed energy [25]

$$\langle E_{\rm rot}\rangle_j=\sum_{j'}\frac{d\sigma}{d\Omega}(j\rightarrow j')\ \Delta\varepsilon_{jj'}\,, \tag{6}$$

where the initial level is taken to be the $j=0$ level and $\Delta\varepsilon_{jj'}$ is the energy gap between the initial and final rotational levels of the target molecule, given in meV. The cross sections were given in $\text{Å}^2\ \text{sr}^{-1}$. The behavior of this quantity is shown in Fig. 9 as a function of a rather broad range of collision energies, from 2.0 eV up to 20.0 eV, and for the whole range of scattering angles. It is a measure of the efficiency of the collisional process in the sense that it tells us, for each scattering angle, the amount of energy which can be lost at that angle by the electrons via the inelastic processes

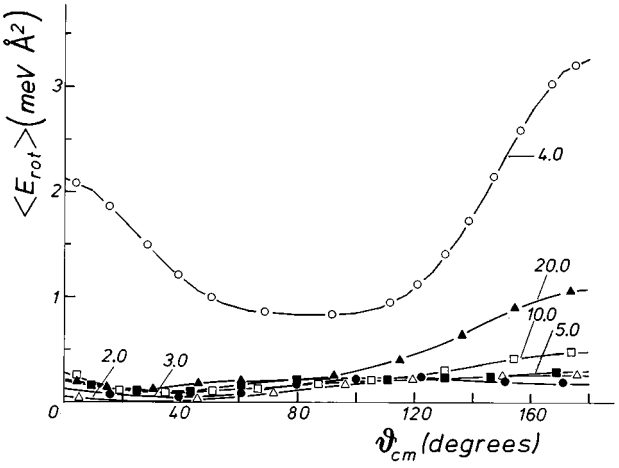

FIG. 9. Computed average energy transfer from Eq. (6) of text with the partial differential cross sections. The $\langle E_{\rm rot}\rangle$ values are plotted as a function of scattering angles and for fixed values of collision energies, as shown for each curve.

that can occur during the collision. We clearly see that the shape resonance around 4.0 eV is markedly more efficient in exciting rotations than any other energy regime and that the d-wave dominant nature of the coupling leads to an angular distribution which is again nearly symmetrical with respect to 90° [24]. All other processes are contributing mostly to the large-angle region and therefore the energy transfer becomes dominated by backward scattering when one moves away from the energy of the Π_u resonance.

Another way of examining the efficiency of the energy transfer processes is to define the average energy transfer via the partial, state-to-state integral cross sections:

$$\langle\Delta E_{\rm rot}\rangle_j=\frac{\sum_{j'}\sigma_{j\rightarrow j'}\,\Delta\varepsilon_{jj'}}{\sum_{j'}\sigma_{j\rightarrow j'}\,.} \tag{7}$$

This quantity is usually given in eV, or in meV, and we have evaluated it for targets in their $j=0$ initial level. The results of the calculations are shown in Fig. 10 and provide us with an interesting insight into the rotational inelasticity at low scattering energies.

(1) The excitation process is rather efficient over the energies examined since its average value is around 0.250 meV, larger than that shown by H_2 and N_2 at the same energies [19].

(2) The range around the Π_u shape resonance shows a strong increase of the excitation efficiency: the $\langle\Delta E_{\rm rot}\rangle$ value reaches more than 0.600 meV at the resonance position, larger than the value found at the resonance position of N_2 [19].

(3) The electrons are able to excite the molecule more efficiently than positrons below the Ps formation and at the same collision energies: recent calculation [26] of $\langle\Delta E_{\rm rot}\rangle$for the CO_2 molecule in collision with positrons found values that were two orders of magnitude smaller than those given here by the electrons.

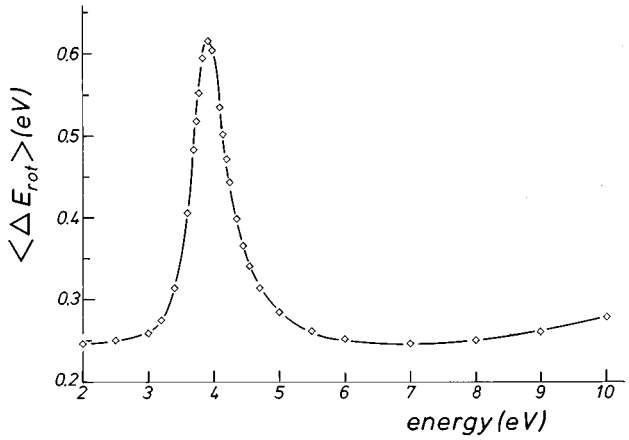

FIG. 10. Computed average energy transfer, Eq. (7) of main text, from the partial integral cross sections. The values of $\langle \Delta E_{\rm rot} \rangle$ are shown as a function of collision energy and in units of meV.

IV. CONCLUSIONS

In the present study we have employed T-matrix elements computed previously [6] within the fixed-nuclei approximation and have transformed them into state-to-state T-matrix elements for rotationally inelastic processes using the ANR scheme. Thus, the actual dynamics included in *ab initio* treatment of all the interaction forces but not their coupling with molecular rotations during the scattering process. This approximation is usually deemed to be realistic at fairly high collision energies but is expected to fail in the regions of resonant scattering. Given the very small spacings of CO_2 rotational levels with low j, however, we expect that such an approach would yield reasonable results for the low-lying excitation processes in the CO_2 molecule even at the low collision energies considered in this work.

We have therefore examined several aspects of the excitation processes and looked at the efficiency of the rotational ''heating'' of the target molecule by collision with electrons. In particular, we have computed first the excitation cross sections from the lower-lying rotational levels with $j=0$, 2, and 4 and found that the $(0\rightarrow 2)$ process is even more probable than the elastic one in the region of the strong Π_u shape resonance of the CO_2 molecule.

The calculations were then extended to excitations with initial-j values from 0 to 10 and the relative importance of the $\Delta j=2$, 4, and 6 processes was examined. It was found that the whole excitation probability increases strongly at the resonance and that the $\Delta j=2$ transition is the one affected the most by the resonance. The suggested physical picture is therefore one in which the dominant partial wave of the resonant state, the $\ell=2$ wave, directly couples the rotational states with $\Delta j=2$ spacings, thereby making these processes the most strongly excited in the resonance region. Furthermore, since partial cross sections at the lower energy have a strong contribution for the Σ_g state [6], then the $\Delta j=2$ transitions are also found to be the most prominent from threshold up to about 4 eV because of the additional couplings from the $\ell=2$, 4, and 6 terms of the interaction which contribute the most to this partial cross section in that energy region.

The analysis of the average energy transfer as an indicator of excitation efficiency [25] suggests that the CO_2 molecule rotations are rather efficiently excited by electron impact in comparison with other, well-studied diatomics like H_2, N_2, and CO, a feature also suggested by earlier model calculations [19].

In conclusion the use of the ANR procedure to yield state-to-state, inelastic partial cross sections for *ab initio* T-matrix elements computed via the FNA modeling shows that one can obtain detailed information from such studies and that they allow us to relate quite directly the observed features of the inelastic cross sections to both the collision dynamics and the structural properties of the target molecule.

ACKNOWLEDGMENTS

The financial support of the Italian National Research Council (CNR) and of the Italian Ministery of University and Research (MURST) is acknowledged. Further financial help of the collaborative EU Network No. ERB. CHRX. CT920013 for a short visit to Rome is also acknowledged (T.S.). Finally, F.A.G. wishes to thank the von-Humboldt-Stiftung for supporting his stay in Professor J.P. Toennies's laboratory in Göttingen when this work was completed.

[1] L. S. Frost and A. V. Phelps, Phys. Rev. **127**, 1621 (1962).
[2] J. J. Lowke, A. V. Phelps, and B. W. Irwin, J. Appl. Phys. **44**, 4464 (1973).
[3] B. R. Bulos and A. V. Phelps, Phys. Rev. A **14**, 615 (1976).
[4] M. Kimura and M. Inokuti, Comments At. Mol. Phys. **24**, 269 (1990).
[5] Y. Itikawa, Phys. Rep. **46**, 117 (1978).
[6] F. A. Gianturco and T. Stoecklin, J. Phys. B **29**, 3993 (1996).
[7] A. Temkin and K. Vasavada, Phys. Rev. **160**, 109 (1967).
[8] W. N. Sams and D. J. Kouri, J. Chem. Phys. **51**, 4809 (1969).
[9] F. A. Gianturco and T. Stoecklin, J. Phys. B. **27**, 5903 (1994).
[10] T. N. Rescigno and A. E. Orel, Phys. Rev. A **24**, 1267 (1981).
[11] F. A. Gianturco, J. A. Rodriguez-Ruiz, and N. Sanna, Phys. Rev. A **47**, 1075 (1993).
[12] F. A. Gianturco, J. A. Rodriguez-Ruiz, and N. Sanna, Phys. Rev. A **52**, 1257 (1995).
[13] D. E. Golden, N. F. Lane, A. Temkin, and E. Gerjuoy, Rev. Mod. Phys. **43**, 642 (1971).
[14] D. M. Chase, Phys. Rev. **104**, 838 (1956).
[15] A. M. Arthurs and A. Dalgarno, Proc. R. Soc. London **256**, 540 (1960).
[16] A. Temkin and E. C. Sullivan, Phys. Rev. Lett. **33**, 1057 (1974).
[17] E.g., see N. Chandra, J. Phys. B **8**, 1953 (1975).
[18] F. A. Gianturco, *The Transfer of Molecular Energies by Collisions* (Springer-Verlag, Berlin, 1979).

[19] M. A. Morrison and N. F. Lane, Phys. Rev. A **16**, 975 (1977).
[20] K. Onda and D. G. Truhlar, J. Phys. B **12**, 283 (1979).
[21] D. Thirumalai, K. Onda, and D. G. Truhlar, J. Chem. Phys. **74**, 6792 (1981).
[22] E.g., see K. Takayanagi and T. Itikawa, Adv. At. Mol. Phys. **6**, 106 (1970).
[23] F. A. Gianturco and F. Schneider, Mol. Phys. **89**, 753 (1996).
[24] D. Andrick and F. Read, J. Phys. B **4**, 389 (1971).
[25] I. Shimamura, Phys. Rev. A **42**, 1318 (1990); **23**, 3350 (1981); J. Phys. B **15**, 93 (1982).
[26] F. A. Gianturco and P. Paioletti, Phys. Rev. A (to be published).